SAR imaging through turbulence

Synthetic aperture radar (SAR) imaging through a turbulent ionosphere

Semyon Tsynkov[1]

[1]Department of Mathematics
North Carolina State University, Raleigh, NC

https://stsynkov.math.ncsu.edu
tsynkov@math.ncsu.edu
+1-919-515-1877

International Conference *Advances in Applied Mathematics*
in memoriam of Prof Saul Abarbanel
Tel Aviv University, December 18–20, 2018

Collaborators and Support

- Collaborators:
  - Dr. Mikhail Gilman (Research Assistant Professor, NCSU)
  - Dr. Erick Smith (Research Mathematician, NRL)
- Support:
  - AFOSR Program in Electromagnetics (Dr. Arje Nachman):
    - ★ Awards number FA9550-14-1-0218 and FA9550-17-1-0230

In memory of Saul Abarbanel

What I plan to accomplish in this talk

- Spaceborne SAR imaging is a vast area:
  - A lot of challenging issues lack attention by mathematicians;
  - Yet any attempt to do a broad overview will be superficial.
- Instead, I would like to:
  - Very briefly outline the key aspects of SAR imaging;
  - Focus on the effect of ionospheric turbulence on spaceborne SAR;
  - Present some recent findings that are unexpected/intriguing;
  - Point out the related misconceptions in the SAR literature;
  - Identify the important questions that require subsequent work.

New research monograph (2017)

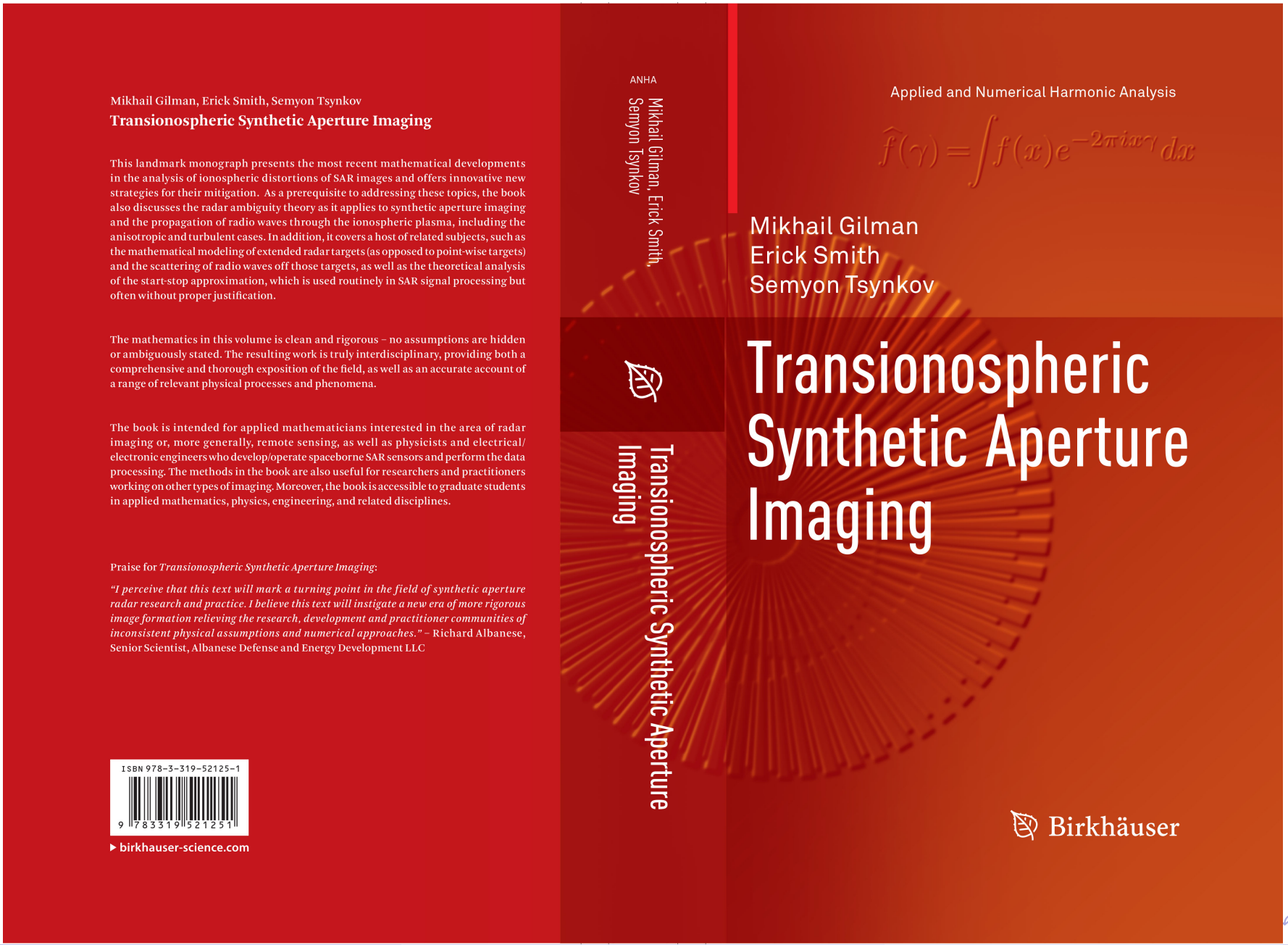

Main idea of SAR

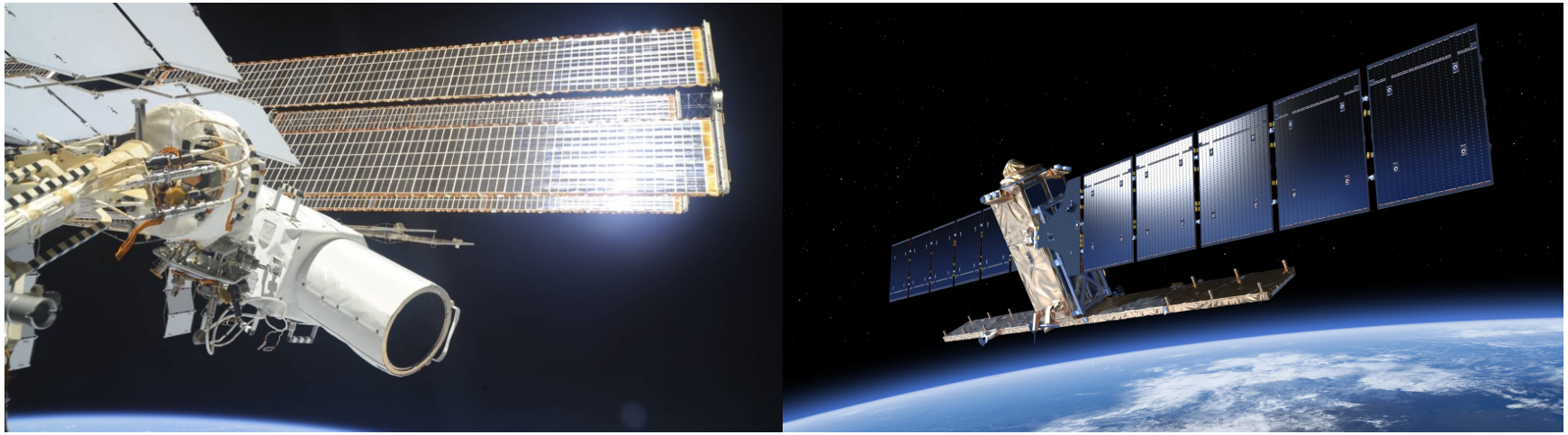

- Coherent overhead imaging by means of microwaves:
  - Typically, P-band to X-band (1 meter to centimeters wavelengh).
- A viable supplement to aerial and space photography.
- To enable imaging, target must be in the near field $\Rightarrow$ instrument size must be very large — unrealistic for actual physical antennas.
- Synthetic array is a set of successive locations of one antenna:
  - Fraunhofer length of the antenna $\frac{2D^2}{\lambda} \ll$ that of the array (aperture);
  - Target in the far field of the antenna is in the near field of the array.

Schematic: monostatic broadside stripmap SAR

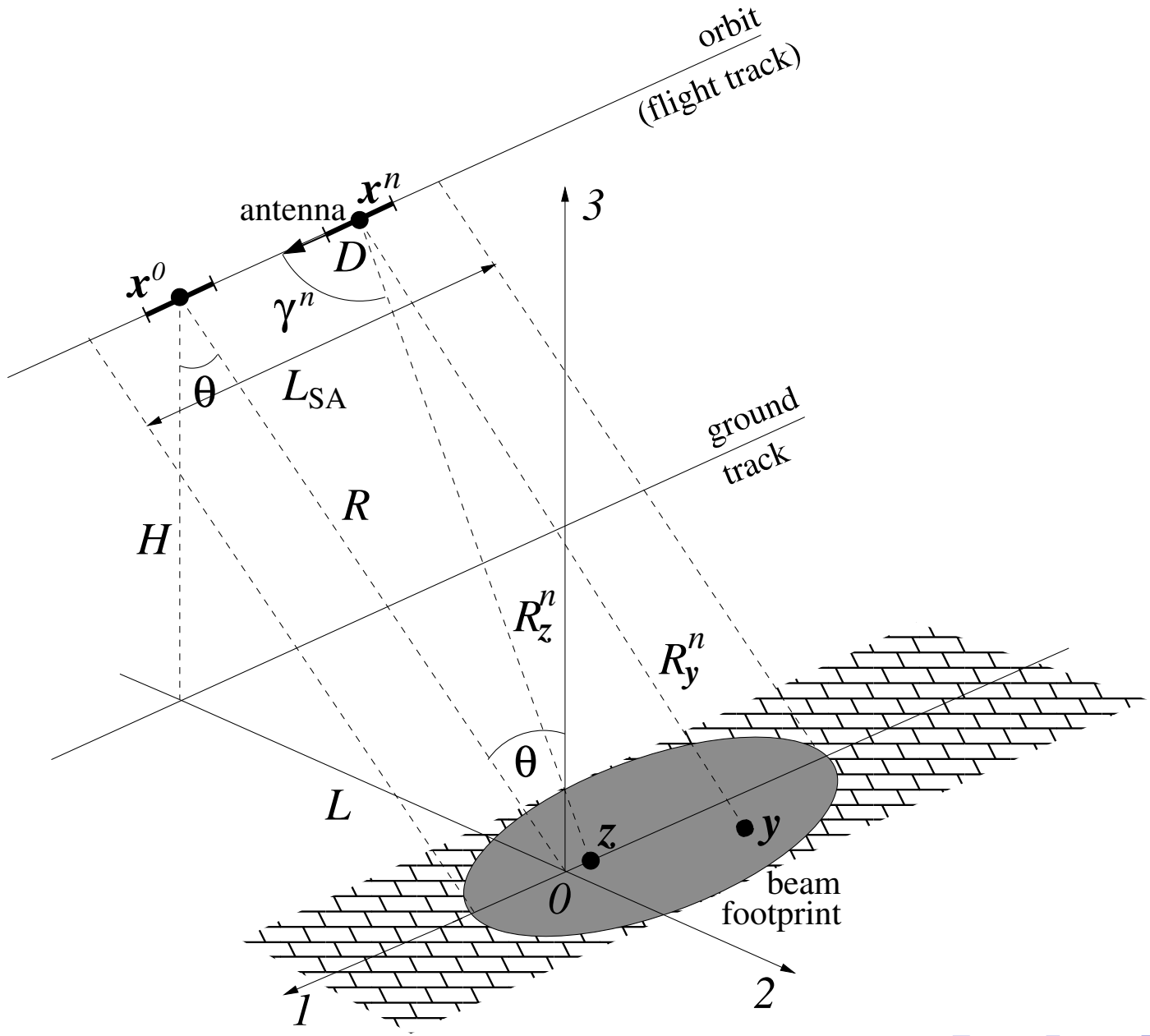

Conventional SAR data inversion

- Interrogating waveforms (fields assumed scalar) — linear chirps:

$$P(t) = A(t)e^{-i\omega_0 t}, \quad \text{where} \quad A(t) = \chi_\tau(t)e^{-i\alpha t^2}.$$

- ω_0 — central carrier frequency, τ — duration, $\alpha = \frac{B}{2\tau}$ — chirp rate.
- Incident field — retarded potential from the antenna at $\boldsymbol{x} \in \mathbb{R}^3$:

$$u^{(0)}(t, \boldsymbol{z}) = \frac{1}{4\pi} \frac{P(t - |\boldsymbol{z} - \boldsymbol{x}|/c)}{|\boldsymbol{z} - \boldsymbol{x}|}.$$

- Scattered field for monostatic imaging (ν — ground reflectivity that also "absorbs" the geometric factors):

$$u^{(1)}(t, \boldsymbol{x}) \approx \int \nu(\boldsymbol{z}) P\left(t - 2|\boldsymbol{x} - \boldsymbol{z}|/c\right) d\boldsymbol{z}.$$

  Obtained with the help of the first Born approximation.
- SAR data inversion: reconstruct $\nu(\boldsymbol{z})$ from the given $u^{(1)}(t, \boldsymbol{x})$.
- The inversion is done in two stages:
  - Application of the matched filter (range reconstruction);
  - Summation along the synthetic array (azimuthal reconstruction).

Generalized ambiguity function (GAF)

- Matched filter ($R_y \equiv |\boldsymbol{y}-\boldsymbol{x}|$, $R_{\boldsymbol{z}} \equiv |\boldsymbol{z}-\boldsymbol{x}|$):

$$I_{\boldsymbol{x}}(\boldsymbol{y}) = \int_{\chi} \overline{P(t-2R_{\boldsymbol{y}}/c)} u^{(1)}(t,\boldsymbol{x})\, dt$$

$$= \int d\boldsymbol{z}\, \nu(\boldsymbol{z}) \underbrace{\int_{\chi} dt\, \overline{P(t-2R_{\boldsymbol{y}}/c)} P(t-2R_{\boldsymbol{z}}/c)}_{W_{\boldsymbol{x}}(\boldsymbol{y},\boldsymbol{z}) \text{ — PSF}}.$$

- Synthetic aperture (determined by the antenna radiation pattern):

$$I(\boldsymbol{y}) = \sum_n I_{\boldsymbol{x}^n}(\boldsymbol{y}) = \sum_n \int W_{\boldsymbol{x}^n}(\boldsymbol{y},\boldsymbol{z})\nu(\boldsymbol{z})d\boldsymbol{z}$$

$$= \int \Big[\sum_n W_{\boldsymbol{x}^n}(\boldsymbol{y},\boldsymbol{z})\Big]\nu(\boldsymbol{z})\, d\boldsymbol{z} = \int W(\boldsymbol{y},\boldsymbol{z})\nu(\boldsymbol{z})\, d\boldsymbol{z} = W * \nu.$$

- $W(\boldsymbol{y},\boldsymbol{z})$ – generalized ambiguity function (GAF) or imaging kernel:

$$W = \sum_n e^{-2i\omega_0(R^n_{\boldsymbol{y}}-R^n_{\boldsymbol{z}})/c} \int_{\chi} e^{-i\alpha 4t(R^n_{\boldsymbol{y}}-R^n_{\boldsymbol{z}})/c} dt.$$

Factorization of the GAF and resolution analysis

- Convolution form $I = W * \nu$ is convenient for analysis:
  - Yet actual processing is done for the entire dataset – not for each $\boldsymbol{y}$.
- Factorized form of the GAF:

$$W(\boldsymbol{y},\boldsymbol{z}) = W(\boldsymbol{y}-\boldsymbol{z}) \approx \tau \mathrm{sinc}\left(\frac{B}{c}(y_2-z_2)\sin\theta\right) N \mathrm{sinc}\left(\frac{k_0 L_{\mathrm{SA}}}{R}(y_1-z_1)\right).$$

- For narrow-band pulses, the factorization error is small: $\mathcal{O}(\frac{B}{\omega_0})$.
- $W(\boldsymbol{y}-\boldsymbol{z}) \neq \delta(\boldsymbol{y}-\boldsymbol{z})$, so the imaging system is not ideal.
- Resolution — semi-width of the main lobe of the sinc$(\,\cdot\,)$:
  - Azimuthal: $\Delta_{\mathrm{A}} = \dfrac{\pi R}{k_0 L_{\mathrm{SA}}} = \dfrac{\pi R c}{\omega_0 L_{\mathrm{SA}}}$; Range: $\Delta_{\mathrm{R}} = \dfrac{\pi c}{B}$.
- What would it be with no phase modulation?
- The range resolution would be $\geqslant$ the length of the pulse τc.
- The actual range resolution is better by a factor of $\dfrac{\tau c}{\Delta_{\mathrm{R}}} = \dfrac{B\tau}{\pi}$.
- $\dfrac{B\tau}{2\pi}$ is the compression ratio of the chirp (or TBP); must be large.

Azimuthal reconstruction

- Linear variation of the instantaneous frequency along the chirp $\omega(t) = \omega_0 + 2\alpha t$ yields the range factor of the GAF:

$$W_{\mathrm{R}}(\boldsymbol{y}, \boldsymbol{z}) = \int_{\chi} e^{-i\alpha 4t(R_{\boldsymbol{y}} - R_{\boldsymbol{z}})/c} dt = \int_{\chi} e^{-2i(\omega(t)-\omega_0)(y_2 - z_2)\sin\theta/c} dt.$$

- In the azimuthal factor, there is a linear variation of the local wavenumber along the array, $k(n) = k_0 \frac{L_{\mathrm{SA}} n}{RN}$:

$$W_{\mathrm{A}}(\boldsymbol{y}, \boldsymbol{z}) = \sum\nolimits_n e^{2ik_0 \frac{L_{\mathrm{SA}} n}{RN}(y_1 - z_1)} = \sum\nolimits_n e^{2ik(n)(y_1 - z_1)}.$$

- Can be attributed to a Doppler effect in slow time n.
- Can be thought of as a chirp of length L_{SA} in azimuth.
- Compression ratio of the chirp in slow time:

$$\frac{L_{\mathrm{SA}}}{\Delta_{\mathrm{A}}} = \frac{2L_{\mathrm{SA}}^2}{\lambda_0}\frac{1}{R} \gg 1, \quad \text{where} \quad \lambda_0 = \frac{2\pi c}{\omega_0}.$$

- $\frac{2L_{\mathrm{SA}}^2}{\lambda_0} \gg 1$ is the Fraunhofer distance of the synthetic array.

Schematic: monostatic broadside stripmap SAR

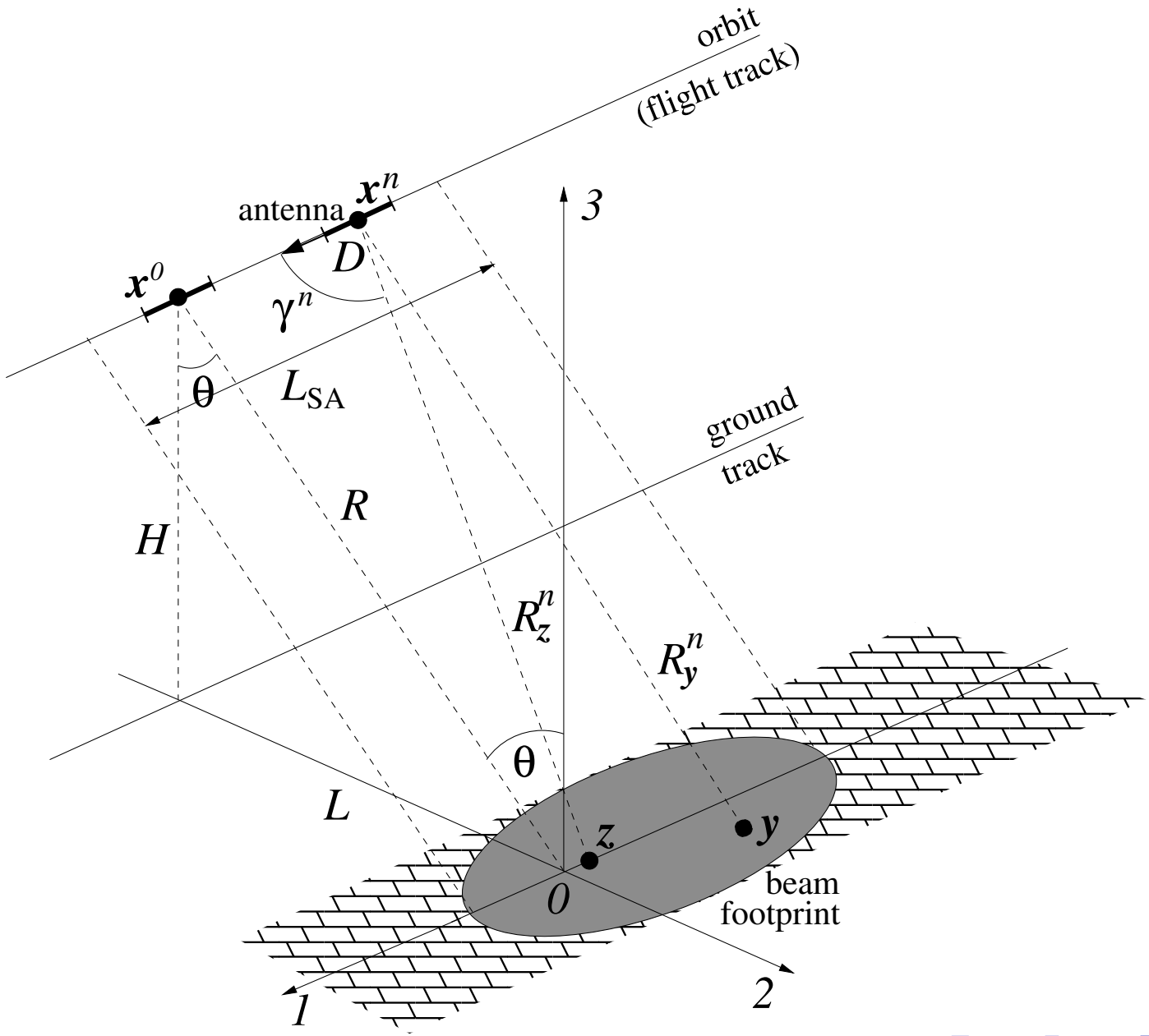

Ionospheric distortions of SAR images

- What the radar actually measures is travel times.
- Distances are determined from times given that c is fixed.
- What if the key assumption "DISTANCE=VELOCITY$\times$TIME" fails?
- EM waves in the ionosphere are subject to temporal dispersion.
- Dispersion relation:

$$\omega^2 = \omega_{\mathrm{pe}}^2 + c^2 k^2,$$

  where $\omega_{\mathrm{pe}}^2 = \frac{4\pi e^2 N_{\mathrm{e}}}{m_{\mathrm{e}}}$ is the Langmuir frequency.
- Group and phase velocities: $v_{\mathrm{gr}} < c$ (delay), $v_{\mathrm{ph}} > c$ (advance).
- Mismatch between the received signal and the matched filter.
- Can be reduced by adjusting the matched filter:
  - One needs real-time total electron content (TEC) and gradients;
  - Can be obtained with the help of dual carrier probing.

Dual carrier probing

- Imaging kernel with mismatch:

$$W(\boldsymbol{y},\boldsymbol{z}) = \sum_n e^{-2i\omega_0(R^n_{\boldsymbol{y}}/c - T_{\mathrm{ph}}(\boldsymbol{x}^n,\boldsymbol{z},\omega_0))} \int_\chi e^{-i\alpha 4t(R^n_{\boldsymbol{y}}/c - T_{\mathrm{gr}}(\boldsymbol{x}^n,\boldsymbol{z},\omega_0))} dt,$$

where

$$T_{\mathrm{ph,\,gr}}(\boldsymbol{x},\boldsymbol{z},\omega_0) = \int_0^{R_{\boldsymbol{z}}} \frac{1}{v_{\mathrm{ph,\,gr}}(s)} ds \approx \int_0^{R_{\boldsymbol{z}}} \frac{1}{c}\left(1 \mp \frac{1}{2}\frac{4\pi e^2}{m_{\mathrm{e}}\omega_0^2} N_{\mathrm{e}}(s)\right) ds = \frac{R_{\boldsymbol{z}}}{\bar{v}_{\mathrm{ph,\,gr}}}.$$

- There are also quadratic phase errors due to change in pulse rate.
- Lead to deterioration of image resolution and sharpness.
- The mismatch also yields a shift of the entire image in range:

$$\Delta R = R_{\boldsymbol{z}} \frac{1}{2}\frac{4\pi e^2}{m_{\mathrm{e}}\omega_0^2}\frac{\mathrm{TEC}}{H}.$$

- Probing on two carrier frequencies, ω_0 and ω_1, creates two shifts.
- Registering two shifted images yields their relative displacement and allows to solve for the unknown TEC.

Transionospheric SAR after the correction

- The new imaging kernel:

$$W(\boldsymbol{y},\boldsymbol{z}) = \sum_n e^{-2i\omega_0 T^n_{\text{ph}}} \int_{-\tau/2}^{\tau/2} e^{-4i\tilde{\alpha}^n T^n_{\text{gr}} t}\, dt,$$

  where $T^n_{\text{ph, gr}} = T_{\text{ph, gr}}(\boldsymbol{x}^n, \boldsymbol{y}, \omega_0) - T_{\text{ph, gr}}(\boldsymbol{x}^n, \boldsymbol{z}, \omega_0)$.

- Factorization:

$$W(\boldsymbol{y},\boldsymbol{z}) \approx \tau N \text{sinc}\left(\frac{B(y_2 - z_2)\sin\theta}{\bar{v}_{\text{gr}}}\right) \text{sinc}\left(\frac{\omega_0 (y_1 - z_1) L_{\text{SA}}}{R\,\bar{v}_{\text{ph}}}\right).$$

- The overall quality of the image is basically restored.
- However, the ionosphere is a turbulent medium.
- Synthetic aperture may be comparable to the scale of turbulence.
- Parameters of the medium will fluctuate from one pulse to another:
  - Using a single correction may still leave room for mismatches.
- One needs to quantify the image distortions due to turbulence:
  - How can one "marry" the deterministic and random errors?

In the presence of turbulence

- The electron number density: $N_{\mathrm{e}} = \langle N_{\mathrm{e}} \rangle + \mu(\boldsymbol{x}), \quad \langle \mu \rangle = 0.$
- The travel times become random:

$$T_{\mathrm{ph,\,gr}}(\boldsymbol{x}, \boldsymbol{z}, \omega_0) = \frac{R_{\boldsymbol{z}}}{\bar{v}_{\mathrm{ph,\,gr}}} \mp \frac{1}{2c} \frac{4\pi e^2}{m_{\mathrm{e}} \omega_0^2} \int_0^{R_{\boldsymbol{z}}} \mu(\boldsymbol{x}(s)) ds \equiv \frac{R_{\boldsymbol{z}}}{\bar{v}_{\mathrm{ph,\,gr}}} \mp \frac{\varphi}{2c}.$$

- Accordingly, the GAF also becomes random (stochastic):

$$W'(\boldsymbol{y}, \boldsymbol{z}) = \sum_n e^{-2i\omega_0 T'^n_{\mathrm{ph}}} \int_{-\tau/2}^{\tau/2} e^{-4i\alpha T'^n_{\mathrm{gr}} t} dt,$$

where

$$T'^n_{\mathrm{ph,\,gr}} = \frac{R^n_{\boldsymbol{y}}}{\bar{v}_{\mathrm{ph,\,gr}}} - T_{\mathrm{ph,\,gr}}(\boldsymbol{x}^n, \boldsymbol{z}, \omega_0) = \frac{R^n_{\boldsymbol{y}} - R^n_{\boldsymbol{z}}}{\bar{v}_{\mathrm{ph,gr}}} \pm \frac{\varphi_n}{2c}.$$

Statistics of propagation

- Correlation function of the medium (turbulent fluctuations):

$$V(\boldsymbol{x}', \boldsymbol{x}'') \stackrel{\text{def}}{=} \left\langle \mu(\boldsymbol{x}')\mu(\boldsymbol{x}'') \right\rangle = \langle \mu^2 \rangle V_r(r) = M^2 \langle N_{\mathrm{e}} \rangle^2 V_r(r),$$

  where $V_r(r) \equiv V_r(|\boldsymbol{x}' - \boldsymbol{x}''|)$ decays rapidly, e.g., $V_r(r) = e^{-r/r_0}$.
- Other short-range correlation functions include Gaussian and Kolmogorov-Obukhov.
- Correlation radius of the medium (outer scale of turbulence):

$$r_0 \stackrel{\text{def}}{=} \frac{1}{V_r(0)} \int_0^\infty V_r(r) dr.$$

- Variance of eikonal describes the magnitude of phase fluctuations:

$$\left\langle \varphi^2 \right\rangle = \left(\frac{4\pi e^2}{m_{\mathrm{e}} \omega_0^2} \right)^2 M^2 \int_0^{R_{\boldsymbol{z}}} \left\langle N_{\mathrm{e}}(h(s)) \right\rangle^2 ds \cdot 2 \int_0^\infty V_r(r)\, dr.$$

- Covariance of eikonal is of central importance: $\langle \varphi_m \varphi_n \rangle$.

Covariance of the eikonal (phase path)

- Affected by statistics of the medium and propagation geometry:

$$\langle \varphi_m \varphi_n \rangle = \left(\frac{4\pi e^2}{m_e \omega_0^2} \right)^2 RM^2 \int_0^1 d\mathfrak{u} \, \langle N_e(h(\mathfrak{u}R)) \rangle^2 \int_{-\infty}^{\infty} ds V_r\left(\sqrt{\mathfrak{u}^2 |\boldsymbol{x}_m - \boldsymbol{x}_n|^2 + s^2} \right).$$

- A common misconception: not accounting for the ionopause.

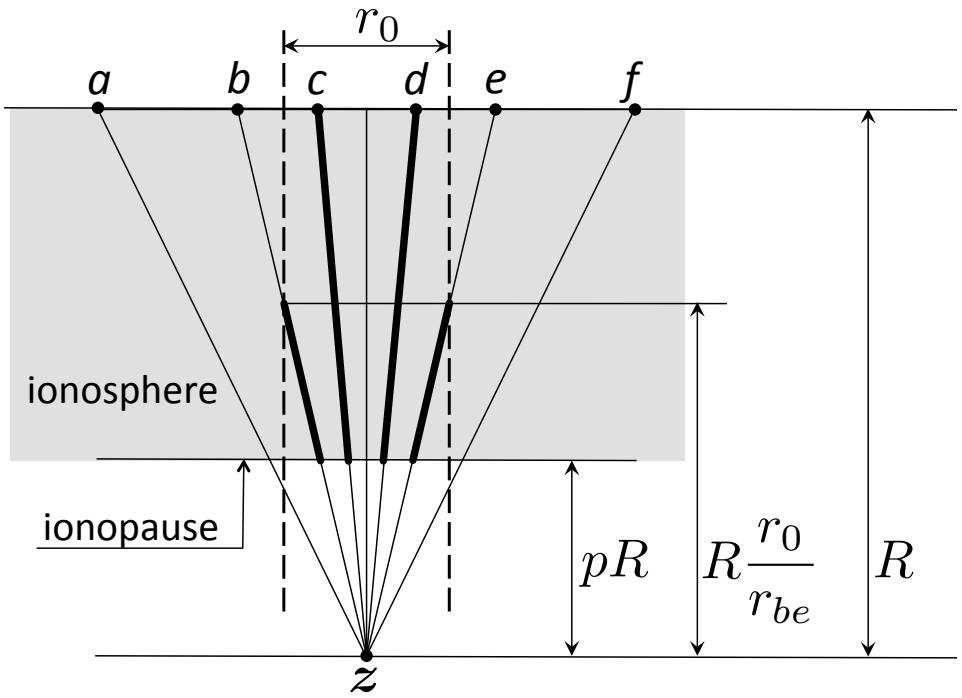

- With no ionopause, $\langle \varphi_m \varphi_n \rangle$ decays slowly even if the correlation function of the medium is short-range.
- With the ionopause, $\langle \varphi_m \varphi_n \rangle$ is also short-range (like V_r) and $r_\varphi \sim r_0$.
- Why is $\langle \varphi_m \varphi_n \rangle$ important?

Stochastic GAF

- Factorization:

$$W'(\boldsymbol{y},\boldsymbol{z}) \approx \tau \mathrm{sinc}\left(\frac{B(y_2-z_2)\sin\theta}{\bar{v}_{\mathrm{gr}}}\right)\cdot\sum_n e^{-2i\omega_0 T'^n_{\mathrm{ph}}}.$$

- For narrow-band signals, the factorization error is small: $\mathcal{O}(\frac{B}{\omega_0})$.
- The effect of turbulence on the imaging in range can be shown to be negligibly small compared to its effect on imaging in azimuth.
- What remains is the sum of random variables over the array.
- Why is it important to know how rapidly the random phase decorrelates along the array?
  - Random phases are normal due to the central limit theorem.
  - Terms in the sum are log-normal: Uncorrelated $\Leftrightarrow$ Independent.
- Statistical dependence or independence of the constituent terms directly affect the moments of the stochastic GAF.

Errors due to randomness

- The mean of the stochastic GAF reduces to the deterministic GAF (subject to extinction $\propto e^{-\pi\langle\varphi^2\rangle/\lambda_0^2}$):
  - The deterministic errors include plain SAR, ionosphere, Doppler, ...
- The errors due to randomness are superimposed on the above:
  - When $r_\varphi \ll L_{\mathrm{SA}}$ and $\sqrt{\langle\varphi^2\rangle} \ll \lambda_0$ (small-scale turbulence with small fluctuations), they are estimated by variance of the stochastic GAF:

$$\sqrt{\sigma^2_{W'_{\mathrm{A}}}} = \sqrt{2}\frac{\omega_0}{c} N \sqrt{\frac{\langle\varphi^2\rangle}{L_{\mathrm{SA}}/r_\varphi}}.$$

  - $\sigma^2_{W'_{\mathrm{A}}}$ quantifies the difference between stochastic and deterministic GAF and accounts for the variation within the statistical ensemble.
- Yet mechanically adding the two types of errors may be ill-advised:
  - In reality, there is a single image rather than an ensemble;
  - For $r_\varphi \ll L_{\mathrm{SA}}$, randomness manifests itself within a single image;
  - For $r_\varphi \gg L_{\mathrm{SA}}$, random phases φ_n within the array are identical:
    - ★ $\sqrt{\sigma^2_{W'_{\mathrm{A}}}}$ is large, yet it basically becomes irrelevant.

Errors due to randomness (continued)

- The case $r_\varphi \gg L_{\mathrm{SA}}$ is very similar to fully deterministic:
  - Image distortions due to randomness can be characterized directly in terms of the azimuthal shift and blurring (expected values),
    - ⋆ NOT as the difference between the stochastic and deterministic GAF;
  - Blurring is significant only for much larger fluctuations than the shift:
    - ⋆ One can have a shifted yet otherwise decent (low blurring) image even for $\sqrt{\langle \varphi^2 \rangle} \gg \lambda_0$.
- On the other hand, in the case $r_\varphi \ll L_{\mathrm{SA}}$, $\sqrt{\langle \varphi^2 \rangle} \gg \lambda_0$ (small-scale turbulence with large fluctuations), the image is completely destroyed (see also [Garnier & Solna, 2013]).
- No "continuous transition" (yet) between the small-scale case and large-scale case.
- Correction of image distortions due to turbulence is a major issue:
  - Current analysis is aimed only at quantification of distortions.

Discussion

- Stochastic GAF and its moments can be computed for a number of commonly encountered models of ionospheric turbulence:
  - In particular, the variance accounts for the difference between stochastic and deterministic GAF.
- The key question is whether this difference should be interpreted as error:
  - Depends on the parameters of the medium and imaging regime.
  - No continuous transition from small to large scale turbulence.
- How can one compensate for image distortions due to turbulence?
  - Is there anything better than the existing autofocus techniques?

Thank you for your attention!